Journal of Emerging Innovations in Engineering (JEIE)
Volume 2, Number 02, June 2026
ISSN: 3110-3375
Open Access: https://jurnal.sutajaya.org/jeie

Synthesis and photocatalytic activity of Fe doped CuO nanoparticles and its kinetics study

Farzana Haider[1,*], Haseeba[2], Kafeel Ahmad Khan[3], Gul Asim Ullah Nabi[4]

[1,2,3,4)]Bacha Khan University, Charsadda, 24420, KPK, Pakistan

Article Info

Article history:
Received May 9th, 2026
Revised June 27th, 2026
Accepted June 29th, 2026

Keyword:
Copper Oxide; Iron-Doped Copper Oxide; Citrus Medica Leaf Extract; Arrhenius Equation; Eosin B Dye.

DOI:
https://doi.org/10.65664/jeie.v2i02.21
Page: 73 - 87

Correspondent Author:
Farzana Haider
Email:
unsty36@gmail.com

ABSTRACT

Nanosized copper oxide and iron doped copper oxide were synthesized using green synthesis method. The samples were characterized using UV-visible spectrophotometer, FT-IR, TGA, EDX SEM and XRD. The particles were irregular yet agglomerated due to interactions between the molecules and the produced NPs. The rate of photocatalytic reaction is greatly affected by the catalyst identity. A maximum degradation of 94.56% for undoped CuO and 97.80% for Fe doped CuO nanoparticles was obtained at 0.03gm of catalyst. The pseudo first order kinetic model best fitted to the experimental data. The Arrhenius equation to the rate constant (k_{App}) was also applied to undoped CuO and Fe doped CuO. The synthesized nanoparticles were cost effective, easy to use and provide greater yield.
.

INTRODUCTION

In 20th century revolutions has made in the ground of nanochemistry and its uses in mechanical industries (Guo et al., 2013), water purification (Mobasser & Firoozi, 2016), food industries (Neethirajan & Jayas, 2011), electronics (Kosmala et. al., 2011), pharmaceuticals and medications (Ali et al., 2016). Nanotechnology has seen significant commercial success in the modern worlds (Khoshnevisan et al., 2019). Because of their small size, nanomaterials offer unique features Metal oxide nanoparticles are produced due to an increase in reactivity and its efficacy (Yaqoob et al., 2020). CuO, also known as cupric oxide, is a p-type semiconductor (Tai et al., 2007). CuO nanoparticles are more steady, flexible, and have a longer shelf life as compared to organic antibacterial agents (Narayan et al., 2018; Kumar et al., 2015). Due to its beneficial characteristics CuO has been widely researched for its variety of potential applications, including electrochemical cells, gas sensors (Zhang et al., 2012), solar cells (Yang et al., 2013), lithium ion batteries (Siddiqui et al., 2020) and catalysis (Waser et al., 2013). Material researchers have used a variety of methods to make CuO NPs, including combustion synthesis (Srivastava et al., 2011), co-precipitation (Rodney et al., 2018), vapour deposition (Liu et al., 2010), sol gel (Blackburn et al., 2016), electrochemical (Usha et al., 2015), electrodeposition (Katwal et al., 2015), radiolysis methods (Wang et al., 2014), wet chemistry route (Alyan et al., 2019), thermal evaporation (Aslani & Oroojpour, 2011), simple chemical precipitation (Huang et al., 2004) and hydrothermal process (Sagadevan et al., 2017). In

ISSN : 3110-3375 DOI: https://doi.org/10.65664/jeie.v2i02.21

recent years, nanomaterials, with a focus on their biomedical and nanotoxicologial effects have been a topic of great development and serious concerns (Desimone, 2019). More recently, the synthesis procedures have been focused by the researchers. Indeed, there is a growing interest in the development of eco-friendly, cost-effective, clean, green, easy to handle, and direct methods for the synthesis of nanomaterials (Chaudhary & Desimone, 2021). The driving forces of this interest is the possibility to diminish energy consumption and avoid toxic or contaminant chemicals. Moreover, the versatility of green chemistry allows producing a wide range of inorganic, organic, and hybrid nanomaterials with numerous promising applications. In green or biogenic synthesis methods, different materials of biological origin, like microorganism, cells, plants or their enzymes or extracts, are employed to synthesize nanomaterials (Gandhi et al., 2020).

The focus is on a greener environment minimizing generated waste, and implementing sustainable processes. For example, the phytosynthesis of nanostructured material is an extremely captivate and challenging approach to all the researchers due to the presence of photochemical agents in the plant extracts (i.e.: carbohydrates, flavonoids, saponins, proteins, amino acids, chromone, steroids, phytol, and terpenoids). The photochemical present in the plant extracts play a key role in improving reduction rate, size, and stabilization by acting as good reducing, surfactants, structure-directing, and capping agents (Sonkusare et al., 2020). In the present work, Fe Doped CuO Nanoparticles were synthesized by green method using Citrus medica leaves extracts, their characterization, kinetics and photocatalytic activity have been investigated.

METHOD

EXPERIMENTAL

Reagents

The chemicals used for undoped and iron doped CuO nanoparticles synthesis were Cu $(NO_3)_3.9H_2O$ and Fe $(NO_3)_2$. The organic compound which was degraded by the above synthesized nanoparticles was Eosin B which has molecular formula ($C_{20}H_8Br_2N_2O_9$). All the chemicals were used of analytical Grade and used without further purifications. Double-distilled water was used in all experiments for preparation of solutions and other purposes.

Leaf Extracts Preparation

Fresh leaves of Citrus medica were collected from district Charsadda. In order to remove dust particles the leaves were washed with double distilled water and dried in shade at room temperature (22-25 °C) for two weeks. After that, using a commercial grinder the leaves were crushed to convert into finely powder form and 200 mL deionized water was added to 20g of finely powdered leaves. Then the mixture was boiled for 40 min at 50 °C in water bath. The extract was cooled down and filtered using filter paper whatman No.1 and for further use stored at 4°C.

Characterization

Double beam UV- visible spectrophotometer (UV-1800 240V, SHIMADZU CORPORATION) was used for determination of dye concentration and wavelength of maximum absorption, FT-IR (Perkin Elmir) spectrophotometer used for the surface adsorption of functional groups, TGA (TGA- 50 100V, Shimadzu Corporation) by monitoring the weight change, it was possible to determine a materials thermal stability and the fraction of volatile components, EDX (Model Inea 200, UK, company oxford) was used for the identification of the elemental composition present in compound, SEM (Model No. JEOL-jsm-5913) used for the high resolution of single nanoparticles and XRD (Model JEOL-300) used to provide information about crystalline structure, nature of phase and crystalline grain size.

Synthesis of Copper oxide (CuO) Nanoparticles

CuO NPs were synthesized by using green synthesis method. 0.2M solution of $Cu(NO_3)_2$ was prepared in 100mL double distilled water under constant stirring at 50 °C temperature. Then leaf extract of Citrus medica was added drop wise to this solution. The solution was homogenized for 3 hr by constant stirring at 2000 rpm using a magnetic stirrer. Finally dark green color precipitate was obtained. The dark green color precipitate gives an indication for the formation of pure CuO NPs. Whatman No.1filter paper was used to filter the precipitates followed by washing with sterilized water. In order to achieve completely dried precipitate, it was then placed in oven for 30 min at 40°C. Moreover, in the pre-heated muffle furnace the manufactured powder nanoparticles were calcinated at

ISSN : 3110-3375 DOI: https://doi.org/10.65664/jeie.v2i02.21

300-400°C for 2 hour to remove impurities and achieve purity. Ultra fine CuO NPs were obtained, which were kept in a sealed container for future usage.

Synthesis of Fe Doped CuO Nanoparticles

Fe-doped CuO NPs were prepared by using green synthesis method. To the as prepared solution of copper nitrate ($Cu(NO_3)_3.9H_2O$) 0.02 M $Fe(NO_3)_2$ solution and citrus medica leaf extract were added drop wise. The solution was homogenized for 3 hour by constant stirring at 2000 rpm using a magnetic stirrer. Finally the colour of the solution was changed and gives an indication for the precipitation of iron doped copper oxide nanoparticles. Whatman No.1 filter paper was used to filter the precipitates. The precipitate was washed 3 times with copious amount of sterilized water and placed in oven for 30 minutes at 40°C. Furthermore, the powder nanoparticles were calcinated in the pre-heated muffle furnace at 300-400°C for 2 hr to remove impurities and achieve purity. Fine black Fe-doped CuO nanoparticles were obtained, which were then preserved in a sealed container for future usage.

Preparation of Dye Solution

The 100ppm stock solution of Eosin B was prepared by dissolving 0.1gm of dye in 1000mL of distilled water and was shaken vigorously. Different concentrations were prepared from stock solution by using dilution formula.

$M_1V_1=M_2V_2$ ……(7)

Photocatalytic Activity

The photocatalytic properties of CuO NPs for Eosin B dye degradation were studied under UV light. For the reaction, dye solution prepared by adding 0.01g CuO NPs in 50 mL (10 ppm), and the reaction mixture was stirred for 10 minutes in the dark. The reaction mixture was then exposed to ultraviolet radiation for 10, 20, 30, 40, 50, and 60 minutes. The experiment was carried out in a UV light box with the adsorption/desorption steadiness being agitated continuously. The Copper oxide nanoparticles were centrifuged out of solution after the reaction, and by using the UV–visible spectrum the dye concentration was determined. The magnitude of the Eosin B absorbance peak (at 517) was measured after a period of time. The light absorption spectrum intensity was used to measure the concentration variation of the Eosin B solution, and the dye degradation was considered as:

$\%Degradation = C_o\text{-}C/C_o \times 100$ ……..(8)

Where C_o and C were the absorbance of the solution before and after the illuminations.

RESULTS AND DISCUSSION

Characterizations

Thermal Gravimetric Analysis (TGA)

The TGA analysis for undoped CuO and Fe-CuO nanoparticles was performed within the same temperature range (25-600^{o}C), although the undoped and Fe doped CuO samples began dehydrating at a lower temperature. This analysis was carried out in the nitrogen environment at warming speed of 15 ^{o}C/min to analyze the weight loss of the synthesized materials (Chaudhary et al., 2019). The reduced weight measured for the undoped sample is around 2.5 percent of the total weight. The weight loss measured for the doped sample is approximately 2.8 percent as shown in Fig. 1 (a, b). It was observed that pure CuO is thermally more stable as compared to Fe-CuO NPs.

ISSN : 3110-3375 DOI: https://doi.org/10.65664/jeie.v2i02.21

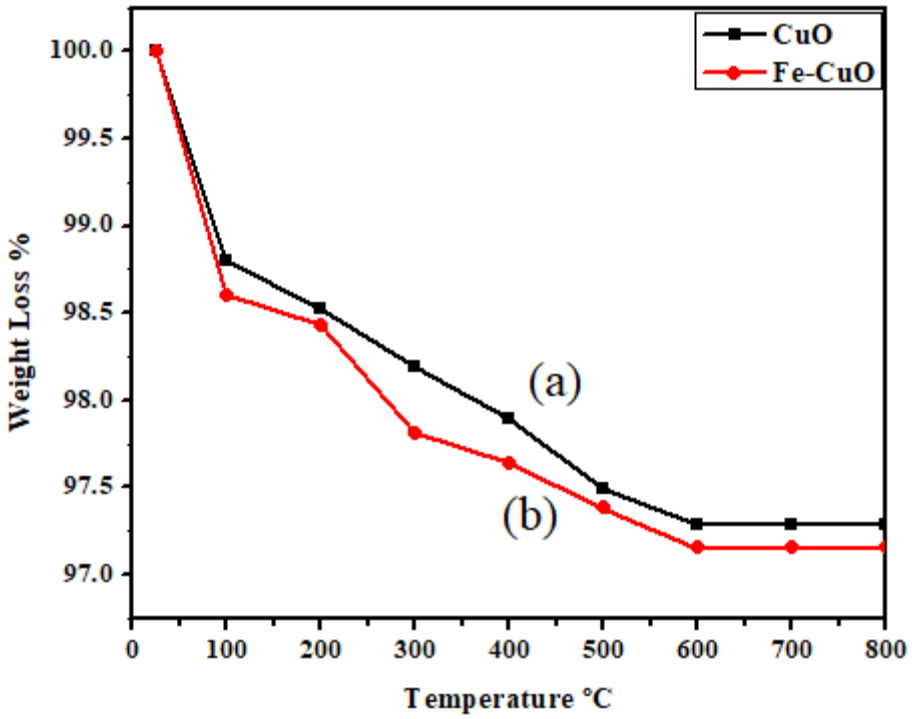

Figure1. Thermal gravimetric analysis of (a) undoped CuO and (b) Fe-CuO nanoparticles.

FTIR Analysis

Figure 2 (a, b) shows the Fourier transform infrared (FT-IR) spectra of the synthesized undoped CuO and Fe-CuO nanoparticles. The bending vibrations of Cu-O and Fe-O bonds match to the absorption bands of metal oxides at 600 and 700 cm^{-1}. The O-H bond is represented by the large peak at 2800-3500 cm^{-1}. The leaf extract has a number of peaks, indicating its complexity. The stretching vibration of C–H bonds is attributed to the bands in the area of 2920 cm^{-1} and 2850 cm^{-1} due to the existence of CH_2 and CH_3 groups in the structure of leaf extract. The peak at 1701 cm^{-1} is caused by carbonyl compound stretching vibrations, indicating the occurrence of fatty acids in the leaf extract. The peak at 1118 cm^{-1} is caused by the stretching vibration of the C–O bond, whereas the peak at 1398 cm^{-1} is caused by stretching vibrations of NO_3, which could be caused by the adhesion of copper nitrate salt, which was utilized as an originator material for the synthesis process (Etape et al., 2018).

ISSN : 3110-3375 DOI: https://doi.org/10.65664/jeie.v2i02.21

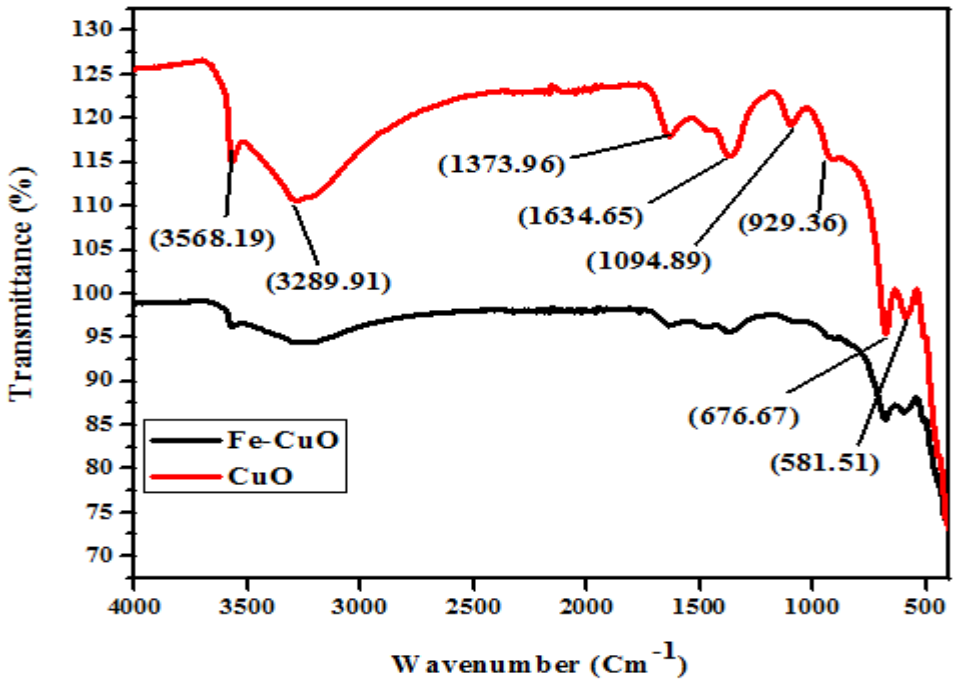

Figure 2. FT-IR Spectra of (a) undoped CuO and (b) Fe-CuO nanoparticles.

Optical Band Gap of CuO and Fe-CuO

The photocatalysts optical characterization was recorded using a UV/V spectrophotometer. The absorbent (A) and sample thickness (t) were used to compute the absorption coefficient (a) associated with the sample's strong absorption zone using the following formula: a 1/4 2.303A/t. The linear component of the plots of $(ahυ)^2$ against the photon energy (h) was extrapolated to determine the optical band gap energy (E_g). The optical band gaps of undoped Copper oxide and Fe doped Copper oxide NPs were determined to be 2.5 eV and 2 eV, respectively as shown in Fig. 3(a, b) (Rajabathar et al., 2021).

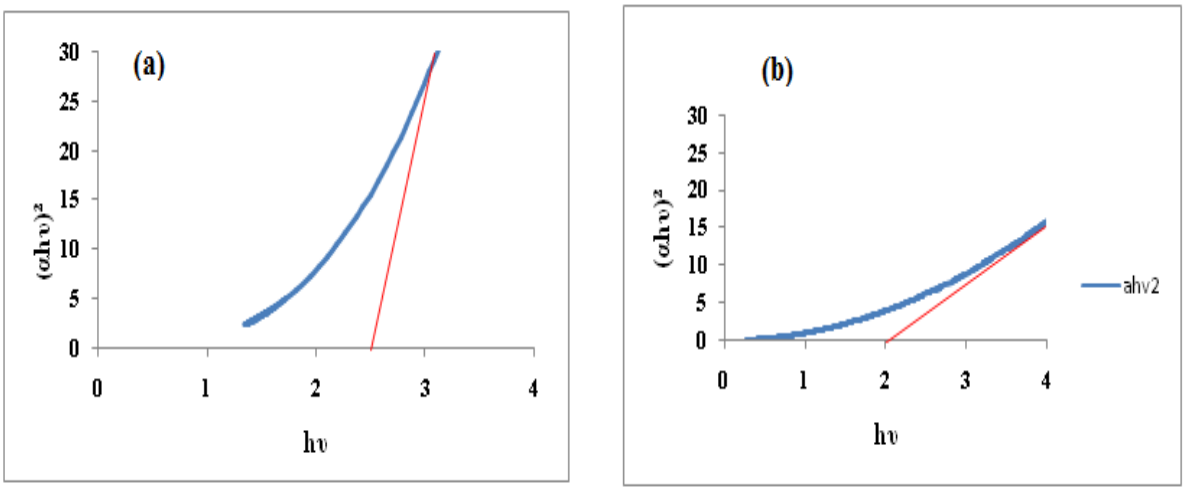

Figure 3. Band gap study for (a) undoped CuO and (b) Fe-CuO nanoparticles.

Scanning Electron Microscopy (SEM)

SEM analysis was used to assess the morphology of the generated undoped Copper Oxide (CuO) and Iron doped Copper Oxide (Fe-CuO) NPs. The SEM picture of undoped CuO exhibits

ISSN : 3110-3375 DOI: https://doi.org/10.65664/jeie.v2i02.21

uneven shape of particles with aggregation as shown in Fig. 4a. In contrast to undoped CuO, Fe doped CuO demonstrates that the particles are uneven and homogeneously scattered as shown in Fig. 4b. As a result of the iron doping, the morphology of the particles improves and particle aggregation decreases.

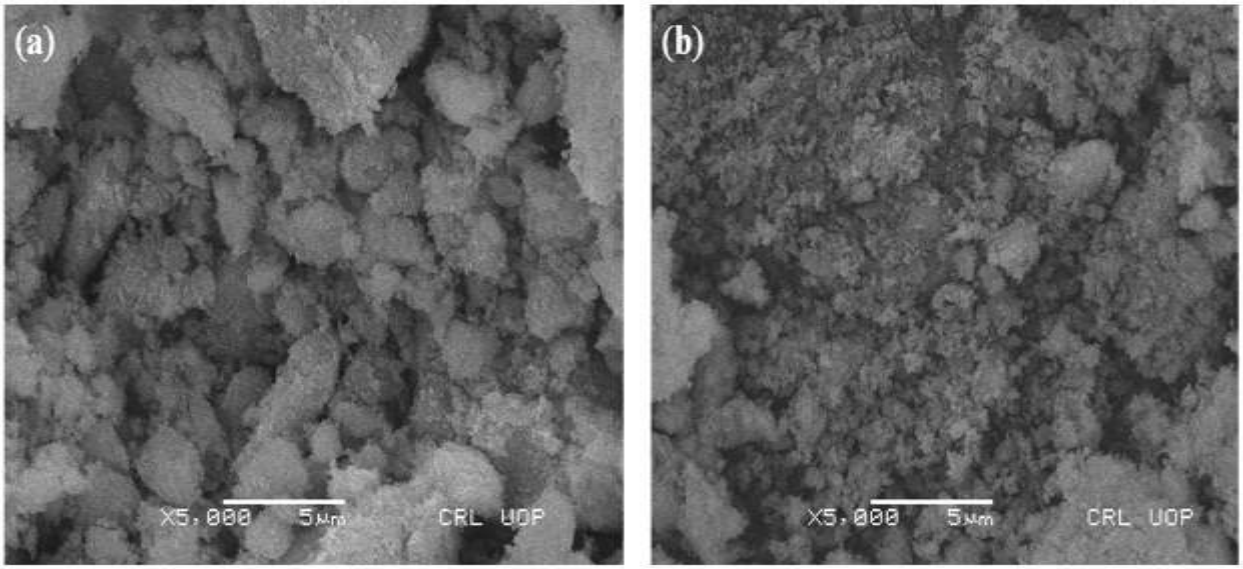

Figure 4. SEM images of (a) CuO and (b) Fe doped CuO nanoparticles.

Energy Dispersive
X-Ray (EDX)

The EDX spectra of green synthesized undoped Copper oxide and iron doped Copper oxide nanoparticles are shown in Fig. 5 (a, b). In the EDX spectra of undoped CuO nanoparticles, the element weight percent of Cu, O, C, and Ca is 88.07 percent, 7.78 percent, 3.65 percent, and 0.51 percent, respectively. The highest concentrations of Cu and O produce prominent peaks, indicating pure copper oxide nanoparticles. In the spectra of Fe doped CuO nanoparticles there was a new peak that represented Fe doping on CuO nanoparticles as shown in Fig. 4b. The dopant Fe weight percentage was about 1.87 percent. Ca peak present in undoped and doped EDX due to plant extract. The bioactive elements found in the Citrus medica plant are indicated by the elemental composition of the undoped CuO and Fe doped CuO patterns.

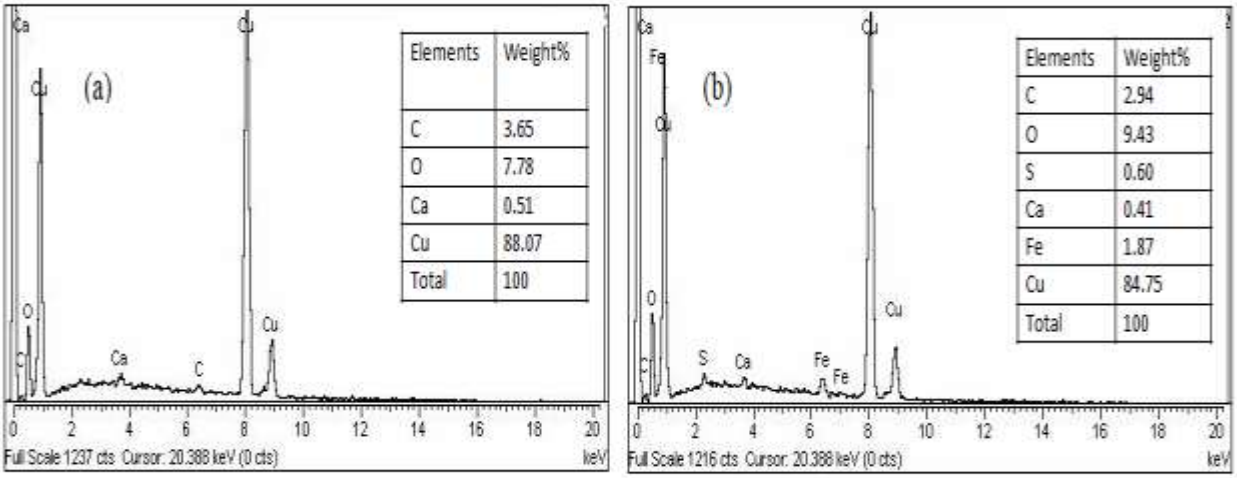

Figure 5. EDX spectra of (a) undoped CuO and (b) Fe doped CuO nanoparticles.

X-Ray Diffraction (XRD)

Figure 6 (a, b) shows the XRD patterns of undoped CuO and Fe-doped CuO NPs. Undoped CuO has two highly intense diffraction peaks at 35.65° and 38.88°, with their orientation along the (-111) and (111) axes, respectively, while Fe doped CuO has two highly intense diffraction peaks at

ISSN : 3110-3375 DOI: https://doi.org/10.65664/jeie.v2i02.21

35.65° and 38.96°, which can define monoclinic structure CuO. Undoped CuO at 32.00°, 48.65°, 53.78°, 58.50°, and Fe doped CuO at 32.34°, 48.89°, 53.86°, 58.59°, corresponding to (110), (-111), (111), (020), and (202). It's the same as card No.80-1917 from the JCPDS. A fine crystallized CuO nanoparticles structure is confirmed by the strong and acute defect spectrum. The crystallite sizes of the CuO and Fe doped CuO crystallites were determined using Scherer's formula to be 17 nm and 14.5 nm, respectively. A nanosized crystallite was found in both samples. Doping of Fe with Copper oxide nanoparticles as dopant has a significant effect on particles size. The diffraction peaks in Fe doped CuO nanoparticles were marginally displaced towards a higher 2 theta angle when compared to undoped CuO. It's possible that this is related to a shift in particle size (Chafi et al., 2018).

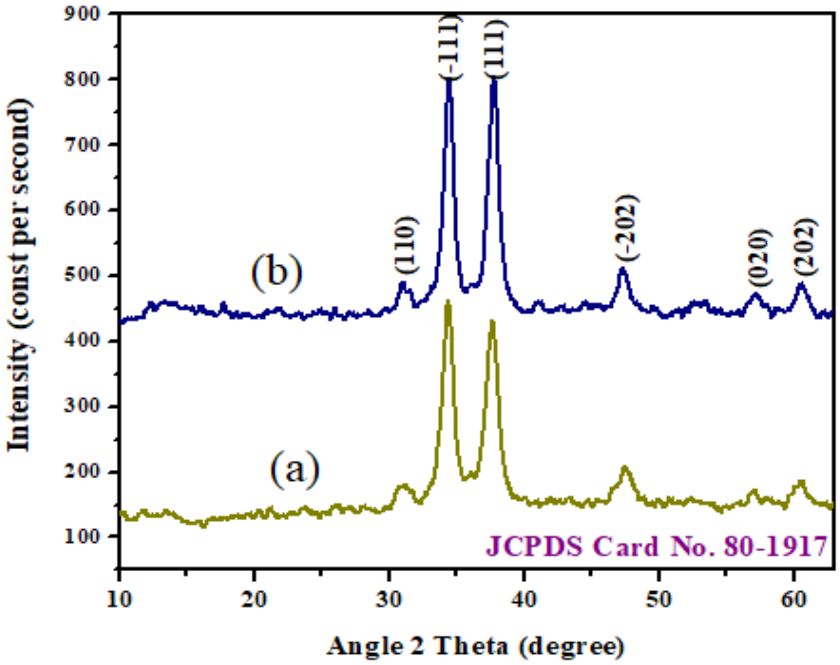

Figure 6. XRD patterns of (a) undoped CuO and (b) Fe doped CuO nanoparticles.

Photocatalytic Degradation of Eosin B Dye

Effect of Contact Time

The photocatalytic degradation of Eosin B was carried out in UV-light at various irradiation times ranging from 10 minutes to 60 minutes. The dye solution was kept in light source after adding 0.03g of undoped CuO and Fe doped CuO catalysts. It has been found during the experiment that the rate of degradation of dye (Eosin B) under the UV-light using undoped CuO and Fe doped CuO catalysts increased with time, kept all parameters constant like, at 0.03g catalyst dose, 10 ppm of dye concentration as shown in Fig. 7 (a, b). The process was repeated for each 10 minutes time interval. The photocatalytic degradation is a photosensitization process, more the irradiation of dye the more will be the generation of electron and holes pairs which is followed by the degradation of dye (Zhao et al., 2009). In case of UV-light the discoloration of dye was observed in initial 10 minutes by using undoped CuO and Fe doped CuO where 44.03% and 61.51% of dye was degraded respectively. With increase in contact time up to 60 minutes the rate of degradation increase until it reach to 89.53% and 94.24% for undoped CuO and Fe doped CuO catalysts respectively.

ISSN : 3110-3375 DOI: https://doi.org/10.65664/jeie.v2i02.21

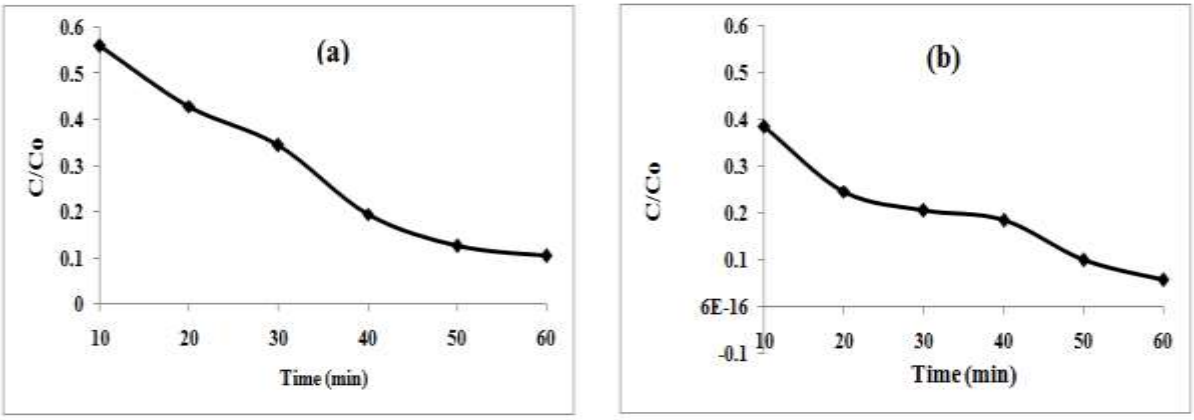

Fig.7. Effect of contact time of (a) undoped CuO and (b) Fe doped CuO NPs on photocatalytic degradation of Eosin B dye at 0.03 gm catalyst, 10 ppm initial concentration of dye, pH 10, 60 ^{o}C and time interval 60 minutes.

Effect of Initial Dye Concentration

The effect of initial concentration of Eosin B dye on the photo catalysis was checked by using concentration ranging from 10ppm-50ppm. The time interval for the degradation was found to be 10 mints as optimum time interval. It was found that the dye degradation decrease with raise in concentration of the dye as shown in Fig. 8 (a, b). It is because of the fact that increasing the concentration of dye resulting in poor degradation was found that the percent degradation decrease as the initial concentration of dye increase. Due to increase in concentration, the intense color of dye did not permit the ultraviolet light to reach the photocatalysts (Behnajady et al., 2006). It was observed that at low concentration of 10 ppm maximum degradation of 89.53% for undoped CuO and 94.24% for Fe doped CuO was obtained.

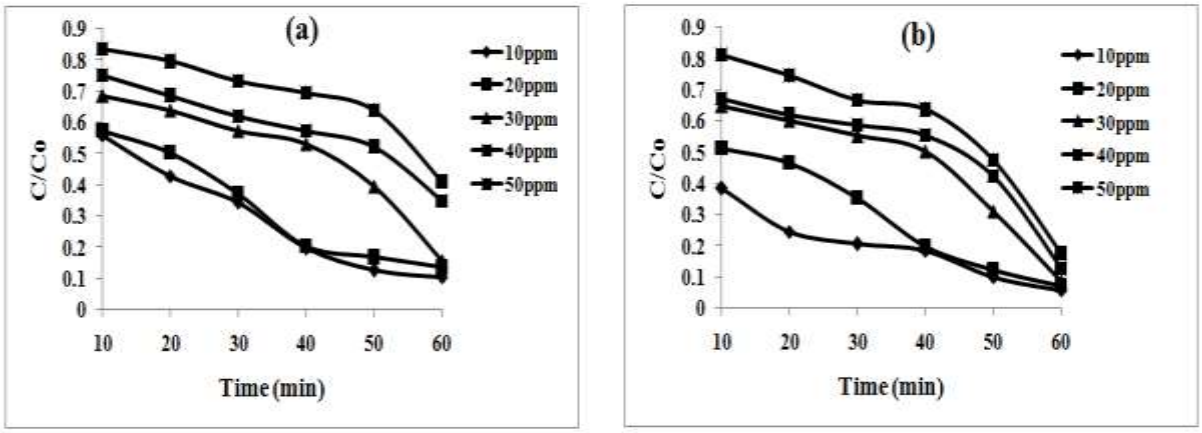

Figure 8. Effect of initial dye concentration of (a) undoped CuO and (b) Fe doped CuO on photocatalytic degradation of Eosin B dye by undoped CuO at 0.03 gm catalyst, pH 10, 60 ^{o}C, dye initial concentration 10 ppm and time interval 60 minutes.

Effect of Catalyst Dose

To obtain an efficient photo catalytic degradation catalyst loading is an important parameter. The amount of catalyst was varied from 0.01gm to 0.04gm for 10 mg/L dye concentration. It was revealed that increasing the catalyst dose up to 0.03gm resulted in a rise in degradation rate as shown in Fig. 9 (a, b). As the amount of catalyst was increased, the degradation rate dropped. The raise in catalytic performance with catalyst dose is due to an increase in the number of active sites present on the catalyst surface; the greater the numbers of active sites, the faster free radicals are produced, and thus, the faster degradation occurs. The decline in catalytic efficiency over a particular point is caused by the turbidity of the slurry solution, which prevents light from passing through the reaction mixture,

ISSN : 3110-3375 DOI: https://doi.org/10.65664/jeie.v2i02.21

lowering the rate of photocatalytic activity (Saharan et al., 2015). A maximum degradation of 94.56% for undoped CuO and 97.80% for Fe doped CuO nanoparticles was obtained at 0.03gm of catalyst. The UV-Visible spectra of photocatalytic degradation of Eosin B using undoped CuO and Fe doped CuO at different catalyst dose is shown in Figure10.

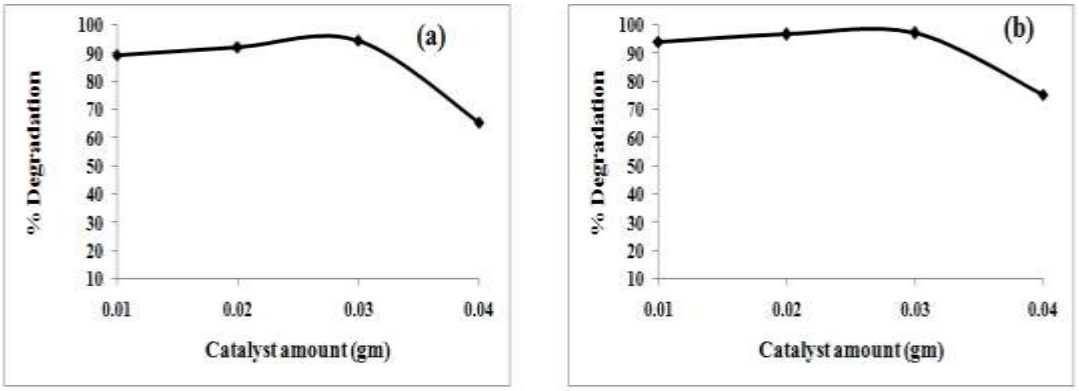

Figure 9. Effect of catalyst dose on photocatalytic degradation of Eosin B dye by (a) undoped CuO and (b) Fe doped CuO at 10 ppm initial concentration of dye, temperature 60 ^{o}C, pH 10 and time interval 60 minutes.

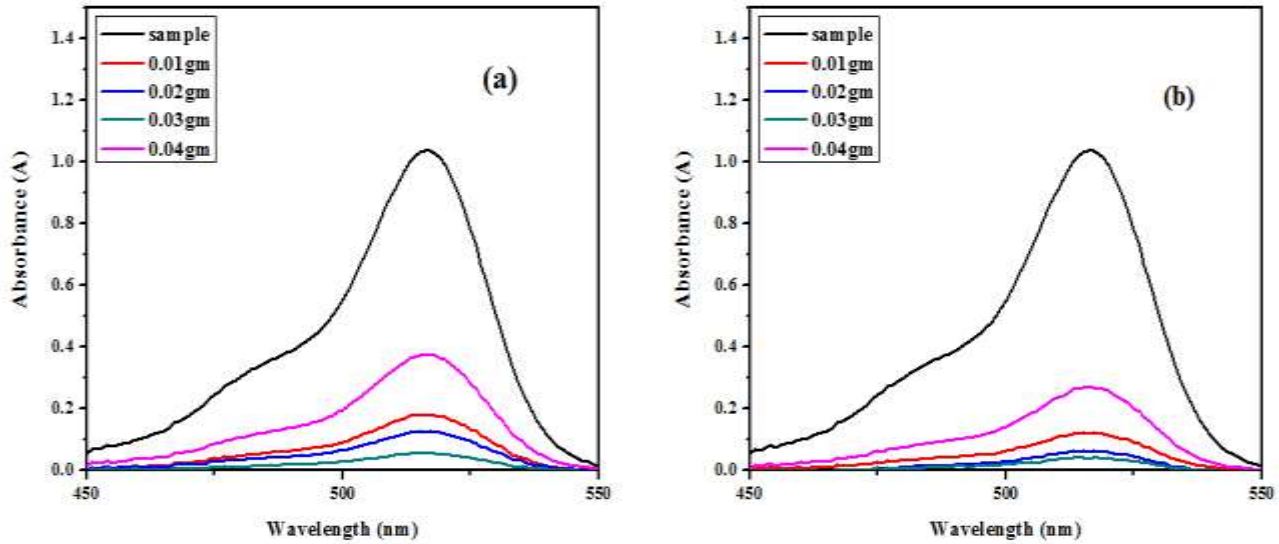

Figure10. UV-Visible spectra of photocatalytic degradation of Eosin B using (a) undoped CuO and (b) Fe doped CuO at different catalyst dose.

Effect of pH

As we know that photocatalytic degradation is highly pH dependent process. pH plays an important role in the formation of hydroxyl radicals. These radicals (·OH) are very unstable in nature and attack on the molecules of dye in the solution (Saeed et al., 2016). In order to study the effect of initial pH on the degradation efficiency of undoped CuO and Fe doped CuO catalysts. In the photo degradation of Eosin B dye the initial pH of the dye in distilled water was determined to be 6.2. Experiment was performed at different pH i.e. pH 2, 4,8,10. The pH values were varied from pH 2 to pH 10 keeping all other parameters constant like at 0.03 gm catalyst dose, at 10ppm dye concentration and at for 1 hour. The pH of solution was adjusted using 0.1 M NaOH and 0.1 M HCl. It was found that as pH increased, the rate of degradation has increased as shown in Fig. 11 (a, b). The highest rate of degradation was found to be 88.59 % for undoped CuO and 93.80 % for Fe doped CuO at pH 10. Fig.12 shows UV-Visible spectra of photocatalytic degradation of Eosin B for both samples at different pH.

ISSN : 3110-3375 DOI: https://doi.org/10.65664/jeie.v2i02.21

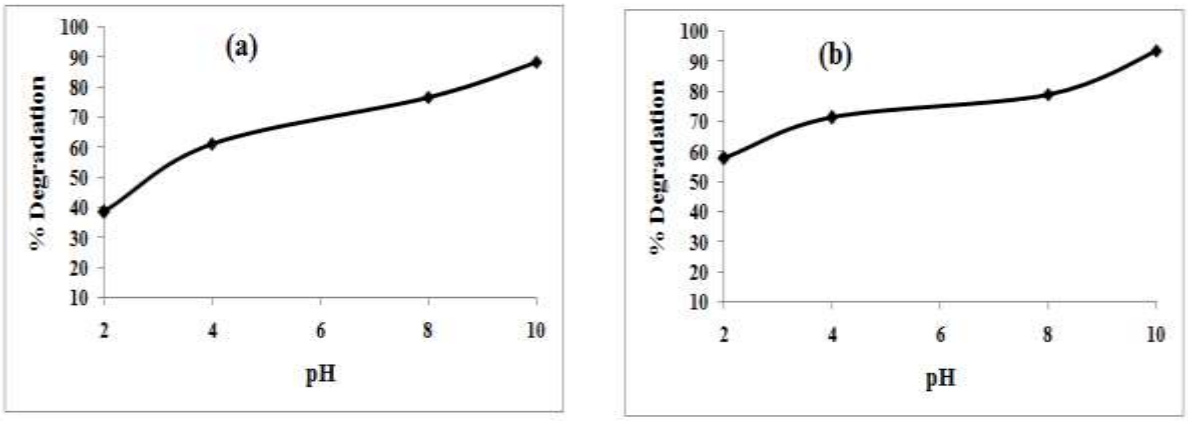

Figure11. Effect of pH on photocatalytic degradation of Eosin B dye by (a) undoped CuO and (b) Fe doped CuO at 0.03 gm catalyst, 10 ppm initial concentration of dye, temperature 60 ^{o}C and time interval 60 minutes.

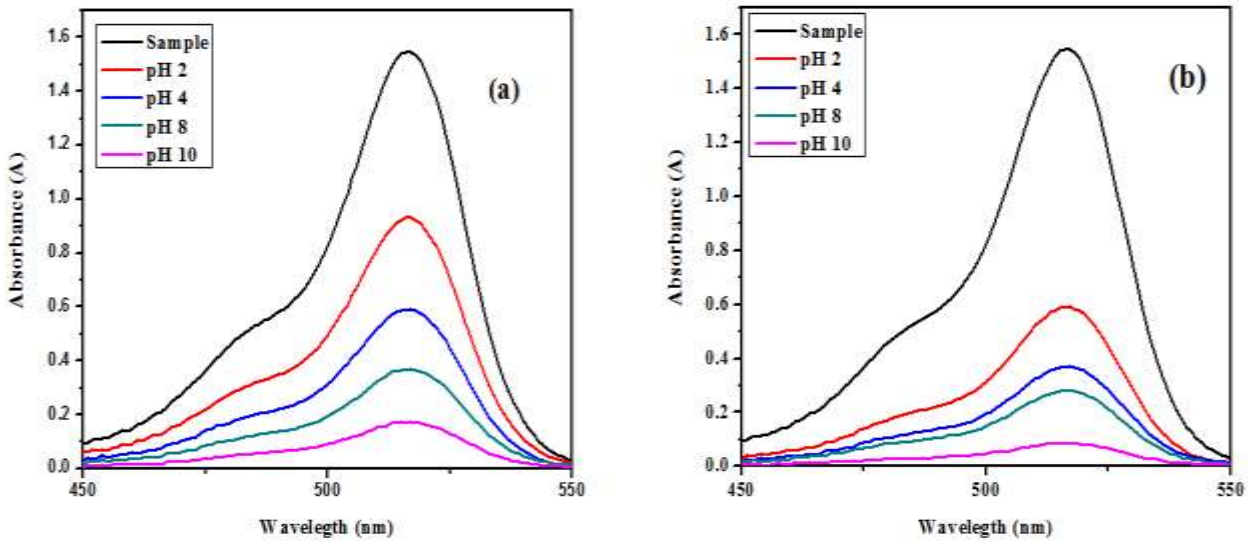

Figure12. UV-Visible spectra of photocatalytic degradation of Eosin B using (a) undoped CuO and (b) Fe doped CuO at different pH.

Effect of Temperature

The temperature has also significant effect on the degradation of Eosin B dye. The dye degradation was carried out at different temperatures (30°C, 40°C and 60°C). It is thought that the collision rate of the substrate molecules increased with rising the temperature, resulting in a rise in the recombination frequency of the electron and hole, resulting in improved degradation efficiency at higher temperatures as shown in Fig. 13 (a, b)(Reza et al., 2017). It was experimentally concluded that with the increase of temperature the degradation also increased and a greatest degradation of 94.52% for undoped CuO and 96.06% for Fe doped CuO was obtained at 60°C.

ISSN : 3110-3375 DOI: https://doi.org/10.65664/jeie.v2i02.21

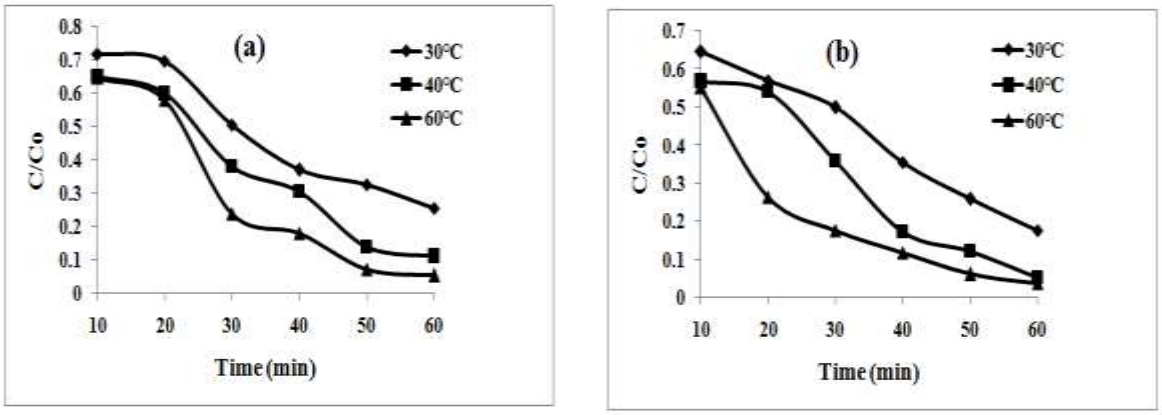

Figure13. Effect of temperature on photocatalytic degradation of Eosin B dye by (a) undoped CuO and (b) Fe doped CuO at 10 ppm initial concentration of dye, 0.03 gm catalyst, pH 10 and time interval 60 minutes.

Kinetics Study

For kinetics study the dye concentration was altered from 10 to 50 mg L^{-1}. To examine the influence of concentration of Eosin B dye on the rate of reaction, 0.03g CuO and Fe doped CuO as photocatalysts was used. Pseudo First order rate constant equation was applied to the concentration data of both nanoparticles, the outcomes of the analysis has been shown in Fig. 14(a) and 14(b), respectively. The values of K_{App} and R at different initial concentration of the dye are shown in Table 1 for undoped CuO and Fe doped CuO respectively. It was observed from the given data that by increasing the dye concentration the rate of degradation decreases. The pseudo first order kinetic model best fitted to the experimental data.

A range of reaction temperatures data of photodegradation was estimated by applying the following equations:

$dc/dt = K_{App} C$ ……. (9)

where k_r and k_{App} are called pseudo-first-order rate constant, respectively.

Eq. (9) can be written in the integrated form as

$\ln (C_o / C) = K_{App} t$ ……(10)

where C_o and C represent initial and final concentration of Eosin B dye.

Table 1. Parameter of first order kinetics equation at different initial concentration using undoped CuO and Fe doped CuO.

Concentration (ppm)		First-Order Kinetics	
		K_{App}	R^2
CuO	10	0.036	0.978
	20	0.031	0.967
	30	0.025	0.747
	40	0.013	0.871
	50	0.013	0.788
Fe-CuO	10	0.041	0.958
	20	0.036	0.951
	30	0.034	0.715
	40	0.027	0.657
	50	0.025	0.724

ISSN : 3110-3375 DOI: https://doi.org/10.65664/jeie.v2i02.21

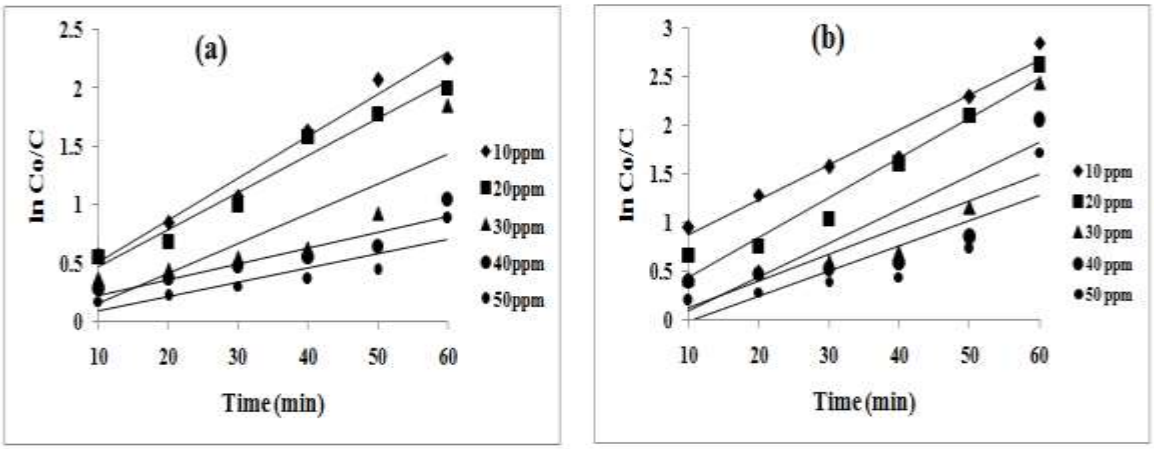

Figure14. Application of pseudo first order kinetics to photodegradation of dye on (a) undoped CuO and (b) Fe doped CuO at different initial concentrations.

Figure 15(a) and 15(b) illustrates the kinetic study of photodegradation of the dye. From the given data it is clear that the rate of photocatalytic reaction is greatly affected by the catalyst identity. For the photodegradation reactions of Eosin B dye over CuO and Fe doped CuO k_{App} along with their correlation coefficient of the pseudo first-order are given in Table 2. It can also be seen that doping CuO with Fe enhanced the reaction slightly in comparison to undoped CuO. The catalytic performance is enhanced by the interaction of Fe with CuO as indicated by these kinetic parameters imitate.

Arrhenius Eq. (11) used to calculate activation energy of the reaction

$K = Ae^{-Ea/RT}$ …… (11)

The logarithmic form of Eq. (11) as

$\ln k = \ln A^{-Ea/RT}$ ……... (12)

A straight line is obtained by interpreting a graph between lnk vs 1/T with slope Ea/R as shown in fig. 16 (a, b). The calculated activation energies from the slopes of graphs were found to be 24.92 and 19.87 KJ/mol for undoped CuO and Fe doped CuO respectively.

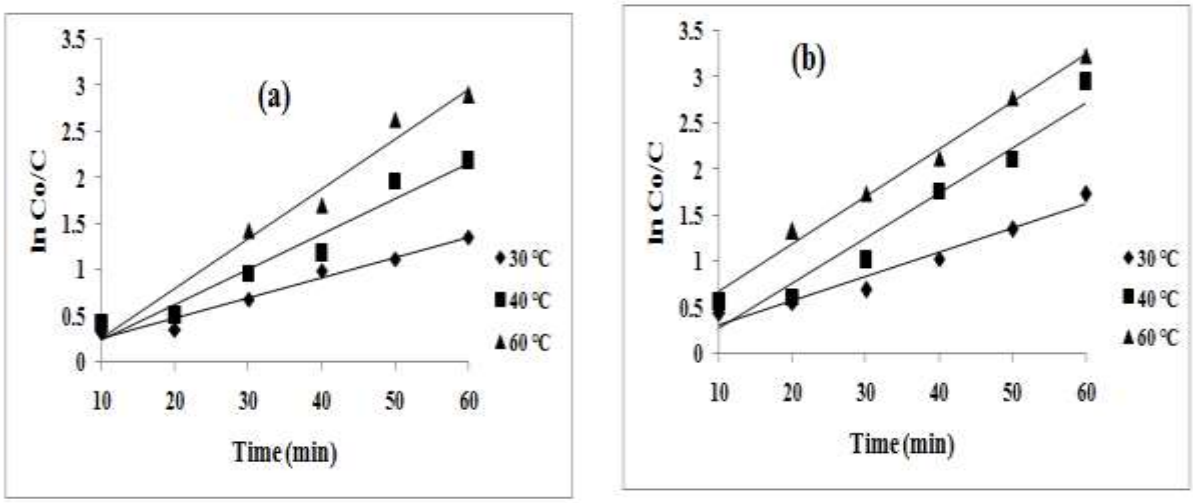

Figure 15. Application of first order kinetics to photodegradation of dye on (a) undoped CuO and (b) Fe doped CuO at different temperature.

ISSN : 3110-3375 DOI: https://doi.org/10.65664/jeie.v2i02.21

Table 2. Parameter of first order kinetics equation of different temperature using undoped CuO.

Temperature (ppm)		First-Order Kinetics		Activation Energy (K.J/mole)
		K_{App}	R^2	
CuO	30	0.022	0.971	24.92
	40	0.038	0.952	
	60	0.051	0.991	
Fe-CuO	30	0.026	0.958	19.87
	40	0.049	0.948	
	60	0.054	0.965	

CONCLUSION

Using leaf extract from Citrus medica, nanosized undoped copper oxide and iron doped copper oxide were synthesized, with average crystallite sizes of 17nm for undoped copper oxide and 14.5nm for iron doped copper oxide. The undoped copper oxide and iron doped copper oxide nanoparticles characterization revealed that they were pure and free of contaminants and that the particles were irregular yet agglomerated due to interactions between the molecules and the produced NPs. At pH 10, the catalysts had outstanding photocatalytic activity against Eosin B textile dye, but their activity increased as the pH increased due to the production of more OH radicals. The application of pseudo first order kinetics model was applied to the concentration and temperature profile data of Eosin B dye degradation. On undoped CuO and Fe doped CuO, the Arrhenius equation to the rate constant (k_{App}) was applied. The synthesized nanoparticles were cost effective, easy to use and provide greater yield.

REFERENCES

Ali, A., Zafar, H., Zia, M., Haq, I., Phull, A. R., Ali, J. S., & Hussain, A. (2016). Synthesis, characterization, applications, and challenges of iron oxide nanoparticles. *Nanotechnology, Science and Applications, 9*, 49–67.

Alyan, A., Abdel-Samad, S., Massoud, A., & Waly, S. A. (2019). Characterization and thermal conductivity investigation of copper-polyaniline nanocomposite synthesized by gamma radiolysis method. *Heat and Mass Transfer, 55*, 2409–2417.

Aslani, A., & Oroojpour, V. (2011). CO gas sensing of CuO nanostructures, synthesized by an assisted solvothermal wet chemical route. *Physica B: Condensed Matter, 406*, 144–149.

Behnajady, M. A., Modirshahla, N., & Hamzavi, R. (2006). Kinetic study on photocatalytic degradation of C.I. Acid Yellow 23 by ZnO photocatalyst. *Journal of Hazardous Materials, 133*, 226–232.

Blackburn, B., Hassan, I., Zhang, C., Blackman, C., Holt, K., & Carmalt, C. (2016). Aerosol assisted chemical vapour deposition synthesis of copper(I) oxide thin films for CO_2 reduction photocatalysis. *Journal of Nanoscience and Nanotechnology, 16*, 10112–10116.

Chafi, Z. F., Bahmad, L., Hassanin, N., Fares, B., Laanab, L., & Mzerd, A. (2018). Characterization techniques of Fe-doped CuO thin films deposited by the spray pyrolysis method. *arXiv preprint arXiv:1807, None*, 1–10.

Chaudhary, R. G., Ali, P., Gandhare, N. V., Tanna, J. A., & Harjeet, D. (2019). Thermal decomposition kinetics of some transition metal coordination polymers of fumaroyl bis (paramethoxy phenyl carbamide) using DTG/DTA techniques. *Arabian Journal of Chemistry, 12*, 1070–1082.

Chaudhary, R. G., & Desimone, M. F. (2021). Synthesis, characterization, and applications of green synthesized nanomaterials. *Current Pharmaceutical Biotechnology, 22*, 722–723.

Desimone, M. F. (2019). Fate and effects of nanomaterials. *Current Pharmaceutical Design, 25*, 3903–3904.

Etape, E. P., Fombuena-Tendo, J., Ngolui, L. J., Namondo, B. V., Yollande, F. C., & Nguimezong, M. B. (2018). Structural characterization and magnetic properties of undoped and Ti-doped ZnO nanoparticles prepared by modified oxalate route. *Journal of Nanomaterials, 1*, 1–8.

Gandhi, A. C., Cheng, C.-L., & Wu, S. Y. (2020). Structural and enhanced optical properties of stabilized γ-Bi_2O_3 nanoparticles: Effect of oxygen ion vacancies. *Nanomaterials, 10*, 1023.

Guo, D., Xie, G., & Luo, J. (2013). Mechanical properties of nanoparticles: Basics and applications. *Journal of Physics D: Applied Physics, 47*, 1–25.

Huang, L. S., Yang, S. G., Li, T., Gu, B. X., Du, Y. W., Lu, Y. N., & Shi, S. Z. (2004). Preparation of large-scale cupric oxide nanowires by thermal evaporation method. *Journal of Crystal Growth, 260*, 130–135.

Katwal, R., Kaur, H., Sharma, G., Naushad, M., & Pathania, D. (2015). Electrochemical synthesized copper oxide nanoparticles for enhanced photocatalytic and antimicrobial activity. *Journal of Industrial and Engineering Chemistry, 31*, 173–184.

Khalid, A., Ahmad, P., Alharthi, A. I., Muhammad, S., Khandaker, M. U., Rehman, M., & Bradley, D. A. (2021). Structural, optical and antibacterial efficacy of pure and zinc-doped copper oxide against pathogenic bacteria. *Nanomaterials, 11*, 451.

Khoshnevisan, K., Maleki, H., Honarvarfard, E., Baharifar, H., Gholami, M., Faridbod, F., & Khorramizadeh, M. R. (2019). Nanomaterial based electrochemical sensing of the biomarker serotonin: A comprehensive review. *Microchimica Acta, 186*, 49–61.

Kosmala, A., Wright, R., & Zhang, Q. (2011). Synthesis of silver nanoparticles and fabrication of aqueous Ag inks for inkjet printing. *Materials Chemistry and Physics, 129*, 1075–1080.

Kumar, P. V., Shameem, U., Kollu, P., Kalyani, R. L., & Pammi, S. V. N. (2015). Green synthesis of copper oxide nanoparticles using Aloe vera leaf extract and its antibacterial activity against fish bacterial pathogens. *BioNanoScience, 5*, 135–139.

Liu, K. L., Yuan, S. L., Duan, H. N., Yin, S. Y., Tian, Z. M., Zheng, X. F., Huo, S. X., & Wang, C. H. (2010). A comparative study on the magnetic properties of Fe-doped nanopowders prepared by sol-gel and co-precipitation method. *Materials Letters, 64*, 192–194.

Mobasser, S., & Firoozi, A. A. (2016). Review of nanotechnology applications in science and engineering. *Journal of Civil Engineering and Urbanism, 6*, 84–93.

Narayan, H., Alemu, H., Maxakaza, L. F., & Jaybhaye, S. (2018). Copper oxide nanoparticles: Synthesis and characterization. *International Journal of Scientific Research in Science, Engineering and Technology, 5*, 43–47.

Neethirajan, S., & Jayas, D. S. (2011). Nanotechnology for the food and bioprocessing industries. *Food and Bioprocess Technology, 4*, 39–47.

Rajabathar, J. R., Al-lohedan, H. A., Arunachalam, P., Issa, Z. A., Gnanamani, M. K., Appaturi, J. N., & Dahan, W. M. (2021). Synthesis and characterization of metal chalcogenide modified graphene oxide sandwiched manganese oxide nanofibers on nickel foam electrodes for high performance supercapacitor applications. *Journal of Alloys and Compounds, 850*, 156346.

Reza, K. M., Kurny, A. S. W., & Gulshan, F. (2017). Parameters affecting the photocatalytic degradation of dyes using TiO_2: A review. *Applied Water Science, 7*, 1569–1578.

Rodney, J. D., Deepapriya, S., Vinosha, P. A., Krishnan, S., Priscilla, S. J., Daniel, R., & Das, S. J. (2018). Synthesis of CuO nanoparticles: Structural and optical properties by sol-gel method. *Optik, 161*, 204–216.

Saeed, K., Khan, I., & Sadiq, M. (2016). Synthesis of graphene supported bimetallic nanoparticles for the sunlight photodegradation of basic green 5 dye in aqueous medium. *Separation Science and Technology, 51*, 1421–1426.

Sagadevan, S., Pal, K., & Chowdhury, Z. Z. (2017). Fabrication of CuO nanoparticles for structural, optical and dielectric analysis using chemical precipitation method. *Journal of Materials Science: Materials in Electronics, 28*, 12591–12597.

Saharan, P., Chaudhary, G. R., Lata, S., Mehta, S. K., & Mor, S. (2015). Ultra fast and effective treatment of dyes from water with the synergistic effect of Ni doped ZnO nanoparticles and ultrasonication. *Ultrasonics Sonochemistry, 22*, 317–325.

Siddiqui, H., Parra, M. R., Pandey, P., Qureshi, M. S., & Haque, F. Z. (2020). Utility of copper oxide nanoparticles (CuO-NPs) as efficient electron donor material in bulk-heterojunction solar

ISSN : 3110-3375 DOI: https://doi.org/10.65664/jeie.v2i02.21

cells with enhanced power conversion efficiency. *Journal of Science: Advanced Materials and Devices, 5*, 104–110.

Sonkusare, V. N., Chaudhary, R. G., Bhusari, G. S., Mondal, A., Potbhare, A. K., Mishra, R. K., Juneja, H. D., & Abdala, A. A. (2020). Mesoporous octahedron-shaped tricobalt tetroxide nanoparticles for photocatalytic degradation of toxic dyes. 5, 7823–7835.

Srivastava, R., Prathap, M. A., & Kore, R. (2011). Morphologically controlled synthesis of copper oxides and their catalytic applications in the synthesis of propargylamine and oxidative degradation of methylene blue. *Colloids and Surfaces A: Physicochemical and Engineering Aspects, 392*, 271–282.

Tai, C. Y., Tai, C. T., Chang, M. H., & Liu, H. S. (2007). Synthesis of magnesium hydroxide and oxide nanoparticles using a spinning disk reactor. *Industrial & Engineering Chemistry Research, 46*, 5536–5541.

Usha, V., Kalyanaraman, S., Thangavel, R., & Vettumperumal, R. (2015). Effect of catalysts on the synthesis of CuO nanoparticles. *Superlattices and Microstructures, 86*, 203–210.

Wang, Y., Jiang, T., Meng, D., Yang, J., Li, Y., Ma, Q., & Han, J. (2014). Fabrication of nanostructured CuO films by electrodeposition and their photocatalytic properties. *Applied Surface Science, 317*, 414–421.

Waser, O., Hess, M., Guntner, A., Novak, P., & Pratsinis, S. E. (2013). Size controlled CuO nanoparticles for Li-ion batteries. *Journal of Power Sources, 241*, 415–422.

Yang, C., Su, X., Wang, J., Cao, X., Wang, S., & Zhang, L. (2013). Facile microwave-assisted hydrothermal synthesis of varied-shaped CuO nanoparticles and their gas sensing properties. *Sensors and Actuators B: Chemical, 15*, 159–165.

Yaqoob, A. A., Parveen, T., Umar, K., & Mohamad Ibrahim, M. N. (2020). Role of nanomaterials in the treatment of wastewater. *Water, 12*, 495.

Zhang, Z., Che, H., Wang, Y., Song, L., Zhong, Z., & Su, F. (2012). Preparation of hierarchical dandelion-like CuO microspheres with enhanced catalytic performance for dimethyldichlorosilane synthesis. *Catalysis Science & Technology, 2*, 1953–1960.

Zhao, L., Ma, J., & Zhai, X. D. (2009). Synergetic effect of ultrasound with dual fields for the degradation of nitrobenzene in aqueous solution. *Environmental Science & Technology, 43*, 5094–5099.